J. Pestic. Sci. **48**(2), 29–34 (2023)
DOI: 10.1584/jpestics.D22-063

JOURNAL OF PESTICIDE SCIENCE

Regular Article

Visualization of azoxystrobin penetration in wheat leaves using mass microscopy imaging

Soichiro Ikuta,[1] Eiichiro Fukusaki[1,2,3] and Shuichi Shimma[1,2,3,*]

[1] *Department of Biotechnology, Graduate School of Engineering, Osaka University, 2–1 Yamadaoka, Suita, Osaka 565–0871, Japan*
[2] *Osaka University Shimadzu Omics Innovation Research Laboratory, Osaka University, 2–1 Yamadaoka, Suita, Osaka 565–0871, Japan*
[3] *Institute for Open and Transdisciplinary Research Initiatives, Osaka University, 2–1 Yamadaoka, Suita, Osaka 565–0871, Japan*

(Received October 18, 2022; Accepted February 2, 2023)

Supplementary material

Fungicides must penetrate the internal tissues of plants to kill pathogenic fungi. Mass spectrometers have been used to confirm this penetration, but conventional mass spectrometric methods cannot distinguish the fungicides in different internal tissues owing to the extraction steps. However, matrix-assisted laser desorption/ionization mass spectrometry imaging (MALDI-MSI) can detect the penetration of fungicides into leaf sections through direct analysis of the sample surfaces. Therefore, the objective of this study was to establish a method for visualizing fungicide penetration in wheat leaf cross sections using MALDI-MSI. The penetration of azoxystrobin from the epidermal to the internal tissue of the leaves was observed. Moreover, azoxystrobin accumulates in the cells around the vascular bundle. This study suggests that MSI can be useful for the evaluation of fungicide penetration in plant leaves.

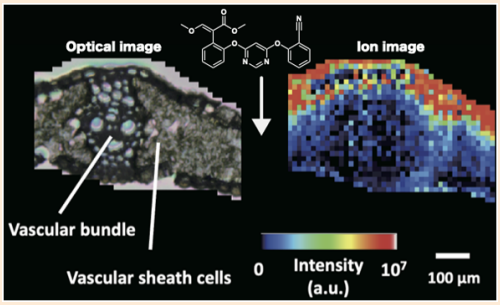

Keywords: mass spectrometry imaging, fungicide, plant, wheat, azoxystrobin.

Introduction

Fungicides have become indispensable for pest control in agriculture. For example, wheat rust has interfered with world wheat production since the domestication of wheat and threatens the global wheat supply.[1)] The annual global losses due to wheat rust are estimated at 4.3–5 billion USD.[2)] Chemical control with fungicides is a method used to avoid yield loss due to these pathogens. However, the repeated use of fungicides can lead to the emergence of resistance in pathogenic bacteria. Therefore, the development of fungicides is ongoing. In the search for lead compounds as fungicides, antimicrobial tests are being conducted on culture media to determine whether candidate lead compounds have fungicidal activity against the target pathogens. Subsequently, candidate compounds that are found to have fungicidal activity are tested for their efficacy against plant pathogens. In some cases, the compound is effective in antimicrobial tests but not in field tests.

One reason for this ineffectiveness is that the candidate compounds did not penetrate the leaf and did not reach the mycelium of the plant pathogen that had extended into the leaf. Plant pathogens, such as *Puccinia triticina*,[3)] which causes wheat leaf rust, and *Puccinia striiformis f.* sp. *Tritici*,[4)] which causes wheat stripe rust, form adherents on the surface of the host leaves and germinate. They penetrate the cuticular layer and epithelium of the leaf and invade its interior, resulting in the death of the host leaf. Therefore, it is necessary to evaluate the effectiveness of pesticide penetration into leaf cross-sections.

Methods using mass spectrometry have been reported to measure pesticide residues after spraying pesticides on foliar surfaces.[5)] Mass spectrometry is an analytical technique that ionizes the molecules contained in a specimen and detects them for qualitative and quantitative analyses of the constituent mol-

* To whom correspondence should be addressed.
E-mail: sshimma@bio.eng.osaka-u.ac.jp
Published online March 23, 2023

ecules. In this method, the surface of a pesticide-applied leaf is rinsed with an organic solvent such as acetonitrile, the leaf is crushed, and the pesticide is removed to evaluate the amount of pesticide penetrating the internal tissues of the leaf. However, information on the distribution of the target component in the leaf is lost during crushing, making it impossible to determine whether the pesticide has penetrated the internal tissues or underside of the leaf.

Alternatively, we propose mass spectrometry imaging (MSI) for the evaluation of the distribution inside wheat leaves. MSI is a method to directly visualize the distribution of target compounds on the surfaces of sample sections by detecting molecules directly.[6] Matrix-assisted laser desorption/ionization (MALDI) is one of the most widely used ionization methods for the analysis of biological samples. Using MALDI-MSI, it is possible to visualize endogenous molecules in central metabolites that constitute the glycolytic system,[7] neurotransmitters,[8] steroid hormones,[9] and exogenous molecules such as pharmaceuticals.[10]

MALDI-MSI has also been used for pesticide tracking imaging and for the visualization of the location of fungicide procymidone residues in cucumber fruits.[11] In addition, the localization of metalaxyl, a fungicide, was visualized in the stems of tomato plant after exposure to its roots.[12] Visualization of metabolite localization in plant leaf cross-sections using MSI has also been reported.[13,14] Three types of embedding materials were used in an example study of *Ginkgo biloba* leaf sections: ice, carboxymethylcellulose (CMC), and gelatin, but delocalization was not observed with embedding using gelatin, indicating that the effect of the different embedding methods is minimal.[13] However, in all those cases, only the distribution of endogenous metabolites in leaf cross-sections was shown, and visualization of the penetration of pesticides applied to leaf surfaces has not been reported.

Strobilurins are a group of widely used agricultural fungicides that are applied to crops mainly by foliar spraying. Azoxystrobin is registered for use in 84 crops in 72 countries, making it one of the most widely used antifungal agents.[15] One reason for the widespread use of this pesticide is its broad antimicrobial spectrum. It is also active against several phytopathogenic fungi. Its mode of action is to bind to the Q_O site of cytochrome *b*, which is located in the inner mitochondrial membrane of fungi and other eukaryotes, thereby blocking electron transfer and inhibiting mitochondrial respiration. Finally, spore germination and motility of migrating spores are inhibited, indicating fungicidal activity.[16] Furthermore, mycelial disintegration of pathogenic fungi has been observed by cryo-scanning electron microscopy studies, indicating that it also has therapeutic effects after infection.[17]

The objective of this study was to establish a method for visualizing the time course of azoxystrobin penetration and tissue localization in wheat leaf cross-sections using MALDI-MSI, and to observe the penetration of the pesticide in wheat leaves after foliar application. Wheat was selected for this study because it is the target crop of azoxystrobin and has the largest cultivated area in the world.[17]

Materials and methods

1. Chemicals

Gelatin, α-cyano-4-hydroxycinnamic acid (α-CHCA), and 2,5-dihydroxybenzoic acid (DHB) were purchased from Merck (Darmstadt, Germany). Methanol, an azoxystrobin standard, formic acid, and 2-propanol were purchased from FUJIFILM Wako Pure Chemicals (Osaka, Japan). Acetonitrile was purchased from Kanto Chemical Co. (Tokyo, Japan). Ultrapure water was prepared using an ultrapure water apparatus (GenPure XCAD UV-TOC, Thermo Fisher Scientific, Waltham, MA, USA).

2. Plant materials

The wheat (*Triticum aestivum* L. cv Apogee) used in the experiment was grown to stage BBCH 39[18] in a greenhouse with a day length of 14 hr and a temperature of 18°C. During this stage, the wheat grows a flag leaf. Because the ability to control harmful fungi in wheat leaves influences production,[19] this leaf was used.

3. Examination of the ionization of azoxystrobin standard

The azoxystrobin and matrix solutions (α-CHCA or DHB) were mixed in equal volumes to obtain a final concentration of 100 ppm azoxystrobin. Azoxystrobin was dissolved in methanol, and α-CHCA solution was prepared with 60% ultrapure water, 30% acetonitrile, 10% 2-propanol, and 0.1% formic acid in a mixture of these solvents to a final concentration of 10 mg/mL. The DHB solution was prepared in 70% methanol to a final concentration of 20 mg/mL.

Sublimation was performed using an iMLayer on a glass slide (ITO-coated glass, Matsunami Glass Industry, Osaka, Japan) coated with indium tin oxide. When α-CHCA was sublimated, the thickness and temperature were set to 0.5 μm and 250°C, respectively, and when DHB was sublimated, the thickness and temperature were set to 0.5 μm and 180°C, respectively. The ionization efficiencies of the two matrices were compared by dropping 0.2 μL of the mixed solution with each sublimated matrix onto ITO-coated glass, allowing it to dry, and performing MSI analysis.

4. Application of azoxystrobin to wheat leaves

Twenty microliters of 1250 ppm (3.1 mM) azoxystrobin solution in methanol was applied to approximately 1 cm^2 of a wheat flag leaf. Then, the area where the solution was applied was sampled. For section preparation, the leaf part was sampled one hour after application. For visualization of penetration, the leaf parts were sampled at one hour, one week, and two weeks after pesticide application.

5. Section preparation method

To prepare sections from frozen wheat leaves, a 10% gelatin solution was used as the embedding agent. The gelatin was dis-

solved in ultrapure water and mixed using a thermomixer (Eppendorf, Hamburg, Germany) at 50°C for 10 min. Cryomold no. 2 (Sakura Finetech Japan, Osaka, Japan) was used as the mold for embedding. The entire wheat leaf was soaked in gelatin solution, or the wheat leaf was floated in gelatin solution. When soaking in gelatin solution, the sample was frozen at −80°C. On the while, when floating the wheat leave on gelatin solution, the surface of the leaf not treated with the fungicide was placed in contact with the solution. After that, the mold was placed in 50 mL centrifuge tubes and quickly frozen in liquid nitrogen. Frozen samples were placed in a cryostat (CM1950, Leica Biosystems, Germany) at −30°C for 2 hr before sectioning. The frozen samples were then mounted in a sample holder using an optimal cutting temperature compound (OCT) to prepare frozen sections with a thickness of 30 μm. Finally, the sections were attached to an ITO-coated glass.

6. Matrix supply to wheat leaf sections

The matrix was applied to wheat leaf sections by sublimation using an iMlayer. The sublimation thickness was 0.5 μm and the temperature was set to 250°C.

7. MSI analysis conditions

An iMScope TRIO (Shimadzu Corporation, Kyoto, Japan) equipped with an atmospheric-pressure MALDI ion source and an ion trap time-of-flight mass spectrometer was used for imaging. All mass and product ion spectra were acquired in positive ion mode using a Nd: YAG laser (355 nm, 1 kHz) for MALDI, with the irradiation frequency set to 80 times and the integration frequency set to 1 time per pixel. The laser irradiation interval was set to 30 μm and the sample and detector voltages were set to 3.5 and 2.1 kV, respectively. After sample analysis, MS images and region of interest (ROI) analyses were performed using Imaging MS Solution (Shimadzu Corporation, Kyoto, Japan) and IMAGEREVEAL MS (Shimadzu Corporation, Kyoto, Japan), respectively. For the ROI analysis, a range was selected at a certain size for each tissue identified by optical images, and a bar graph was created based on the mean value of the intensity obtained from each tissue. Student's *t*-test was used to examine significant differences between the means of two groups that did not correspond to each other, and ANOVA was used to examine significant differences between the means of three or more groups.

Results and discussion

1. Ionization of azoxystrobin using MALDI

Two types of matrices were compared for the detection of azoxystrobin. When a mixture of the azoxystrobin standard and each matrix was dropped onto an ITO glass slide, the strongest peak appeared at *m*/*z* 404.12 (Fig. 1). The exact mass of azoxystrobin is 403.117, and it is considered that azoxystrobin was detected as a hydrogen adduct at *m*/*z* 404.12. Therefore, in this study, the detection intensity at this *m*/*z* was used to visualize the azoxystrobin distribution. Furthermore, when α-CHCA was used as the matrix (Fig. 1A), the intensity of the peak was higher than when DHB was used as the matrix (Fig. 1B). Therefore, α-CHCA was selected as the matrix and used in all subsequent experiments.

2. Wheat leaf sections

After wheat leaves were embedded in the gelatin solution, frozen sections were prepared. Azoxystrobin was then detected and visualized using MSI, and the results were merged with optical images (Fig. 2A). Optical micrographs of the section showed that upper epidermal cells, mesophyll cells, vascular bundle and lower epidermal cells could be distinguished. However, azoxystrobin applied to the surface of a wheat leaf was detected on the embedding agent section, not on the wheat leaf section. By soaking the wheat leaves applied with azoxystrobin in the gelatin solution, it is thought that the azoxystrobin diffused into the gelatin solution. Moreover, azoxystrobin was detected along the edge of the embedding agent section, probably because the water in the gelatin solution was slowly frozen in the −80°C freezer. Therefore, to prevent the fungicide on the leaf surface from diffusing into the gelatin solution, wheat leaves were floated in the gelatin solution and then frozen quickly in liquid nitro-

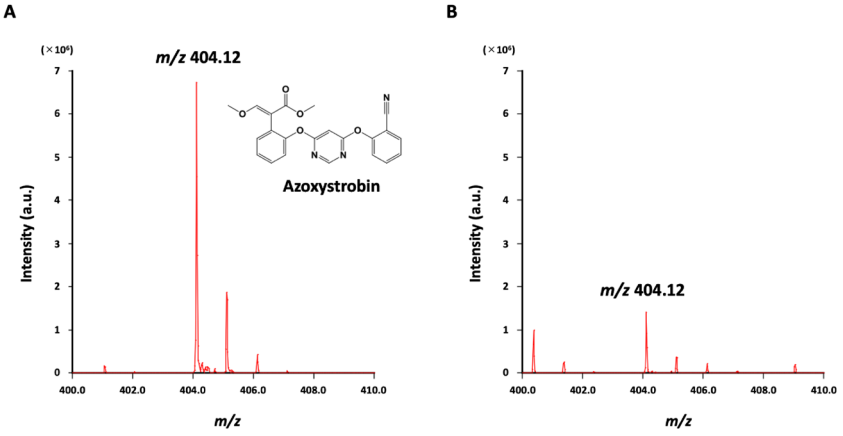

Fig. 1. Comparison of the ionization efficiency of azoxystrobin standard using two types of matrices. (A) α-CHCA solution (B) DHB solution

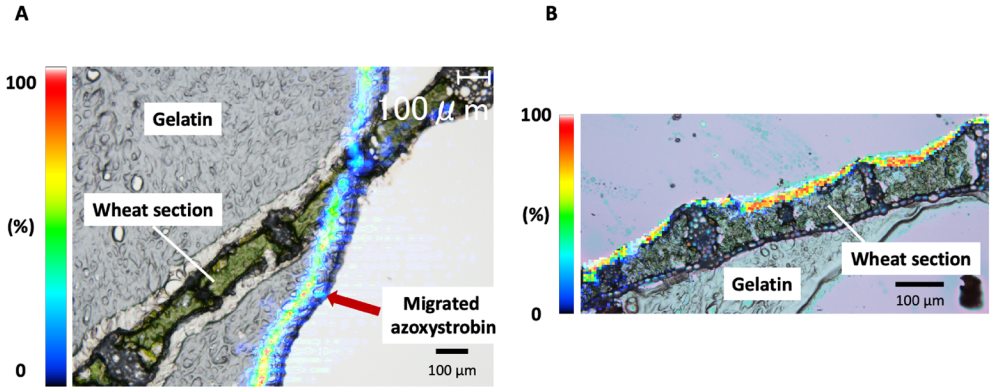

Fig. 2. Visualization of azoxystrobin in wheat leaf cross-sections using two embedding methods. (A) The entire wheat leaf was soaked in gelatin solution. (B) The wheat leaf was floated in gelatin solution.

gen. Azoxystrobin was detected along the upper epidermal cells of the wheat leaf, as shown in Fig. 2B, preventing azoxystrobin from leaking into the gelatin solution.

3. *Visualization of azoxystrobin penetration in wheat leaf sections*

To observe azoxystrobin penetration, the distribution of azoxystrobin (*m*/*z* 404.12) was visualized on wheat leaves at one hour, one week, and two weeks after azoxystrobin application (Fig. 3A). The results show that azoxystrobin was mainly detected in the upper epidermal cells of the fungicide-treated leaves after one hour of application, whereas it penetrated the mesophyll cells and vascular bundle after one week. From the results of each time course, ROIs were selected from the upper epider-

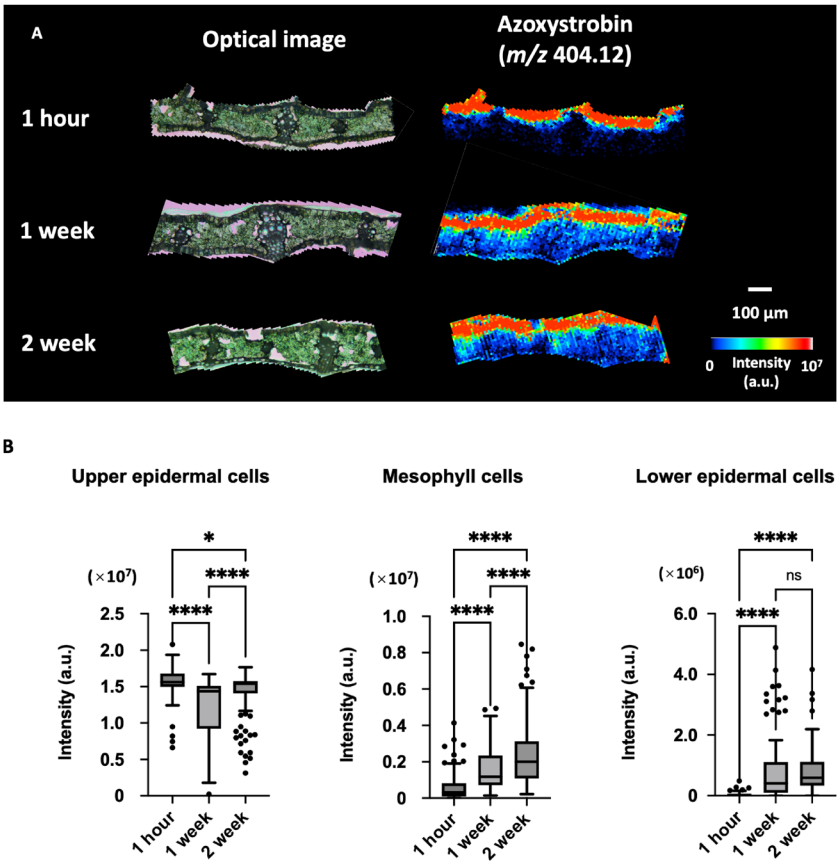

Fig. 3. (A) Azoxystrobin distribution (*m*/*z* 404.12) was visualized on wheat leaves one hour, one week, and two weeks after azoxystrobin application. (B) Box plots from ROIs selected from the upper epidermal cells and the mesophyll cells, and the lower epidermal cells in each time course results. Asterisks represent the differences at confidence levels of $*p<0.05$ and $****p<0.0001$

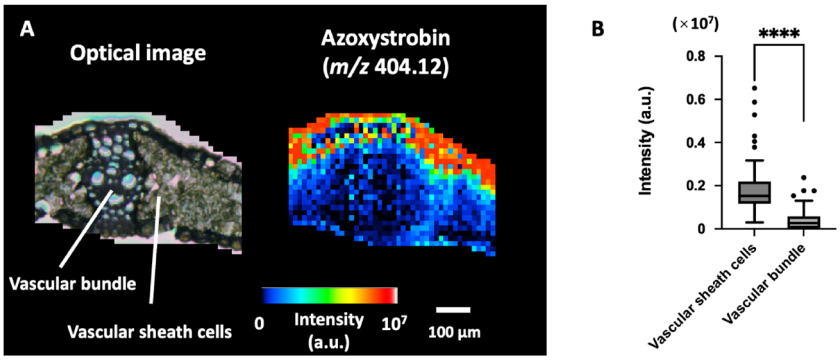

Fig. 4. (A) Azoxystrobin distribution (*m*/*z* 404.12) was visualized in the vascular bundle and the vascular sheath cells of wheat leaves one week after azoxystrobin application (B) Box plot from ROIs selected from the vascular bundle and the vascular sheath cells in the MSI results. The asterisk represents the difference at confidence level of ****$p<0.0001$.

mal cells and the mesophyll cells, and the lower epidermal cells on the reverse side of azoxystrobin application. The *m*/*z* 404.12 peak intensity detected from the laser-irradiated points (60 points) in each ROI was plotted and a box plot is shown in Fig. 3B. The results showed that the intensity of azoxystrobin detection in the upper epidermal cells decreased from one hour to one week, whereas the detection intensity increased in the mesophyll cells and lower epidermal cells. From one to two weeks later, the intensity of azoxystrobin detection in the upper epidermal cells decreased and that in the mesophyll cells increased. These results confirmed the penetration of azoxystrobin from the upper epidermal cells to the mesophyll cells and the lower epidermal cells, although azoxystrobin was still detected in the upper epidermal cells without penetrating probably because of the densely lined cell layers.

In the image results one week after azoxystrobin application, we noted that azoxystrobin accumulated in the vascular sheath cells rather than in the vascular bundle of the leaf (Fig. 4A). Therefore, two ROIs were selected based on the vascular bundle and vascular sheath cells in the image results, and the peak intensity at *m*/*z* 404.12 detected from the laser-irradiated points (25 points) in each ROI, was plotted (Fig. 4B). Significant differences were observed in the peak intensities of ROIs. Furthermore, the reproducibility of this result was confirmed (Fig. S1).

There are three possible reasons for this difference in distribution. First, it is easier for the fungicide to penetrate the surrounding mesophyll cells than the vascular bundle from the upper epidermal cells. The vascular bundles in wheat leaf cross-sections are surrounded by densely packed cells called the vascular sheath cells and extensions. In vascular sheath extensions, the horizontal diffusion of water molecules is restricted,[20] and azoxystrobin is also inhibited from penetrating the cells in these tissues. This suggests that accumulation in the vascular bundle was lower than that in the surrounding vascular sheath cells.

Second, azoxystrobin is transported through vascular bundles. It has been reported that azoxystrobin permeates the xylem of vascular bundles.[15] This suggests that azoxystrobin that penetrated the vascular bundle was transported through the xylem of the vascular bundle, and thus did not accumulate in the vascular bundle.

The third mechanism is thought to be due to the metabolism of the fungicide in the vascular bundle. Azoxystrobin is metabolized by cytochrome P450.[21] Several cytochrome P450s were strongly detected in the leaf vascular system of *Arabidopsis thaliana* using GUS staining,[22,23] suggesting that cytochrome P450s involved in azoxystrobin metabolism may also metabolize azoxystrobin in the vascular system. Although MSI can be used to investigate the localization of compounds using the intensity derived from the fungicide, it can only be used to investigate metabolites that can be detected using mass spectrometer. To better elucidate these biological phenomena, it must be combined with other methods such as gene expression analysis and enzyme activity measurements related to the fungicide metabolism.

Conclusions

In this study, wheat leaf sections were prepared and visualized. To date, several studies have reported the preparation of frozen plant leaf sections for MSI.[13,14] However, all these reports embedded the entire leaf and were not suitable for the visualization of foliar-applied fungicides because of the leakage caused by the embedding agent. In this study, a fungicide applied to the leaves of wheat plants were visualized by floating the leaves in embedding medium. The distribution of the fungicide azoxystrobin in wheat leaf cross-sections was visualized using the azoxystrobin-derived peak (*m*/*z* 404.12), and we confirmed that azoxystrobin reached the entire leaf one week after application. This is the first report on the visualization of azoxystrobin localization in leaf cross-sections. Furthermore, more azoxystrobin accumulated in vascular sheath cells around vascular bundles inside the leaves than in the vascular bundles. This suggests that MSI can be used to analyze the distribution of fungicides in plant leaves. For example, when developing fungicides, it can be useful to determine the optimal formulation by comparing the fungicide penetration into the leaf using multiple formulations to enhance the uptake of fungicides into the plant body. In conclusion, MSI can be applied for the analysis of fungicide distribution in plants because it can selectively analyze the distribution of fungicides

without special labeling.

Acknowledgements

We would like to thank Prof. Iida of the Shimadzu Institute for Analytical Innovation and Collaborative Research, Osaka University, for allowing us to use the iMScope TRIO and iMLayer in the course of this research. This study was partially supported by the Institute for Open and Transdisciplinary Research Initiatives. This study will be included in a dissertation submitted by Soichiro Ikuta to Osaka University to partially fulfil the requirements for his doctoral degree.

Electronic supplementary materials

The online version of this article contains supplementary material (Fig. S1) which is available at https://www.jstage.jst.go.jp/browse/jpestics/.

References

1) A. P. Roelfs, R. P. Singh, and E. E. Saari: "Rust Diseases of Wheat Concepts and Methods of Disease Management," International Maize and Wheat Improvement Center, El Batan, 1992.
2) M. Figueroa, K. E. Hammond-Kosack and P. S. Solomon: A review of wheat diseases—A field perspective. *Mol. Plant Pathol.* **19**, 1523–1536 (2018).
3) M. D. Bolton, J. A. Kolmer and D. F. Garvin: Wheat leaf rust caused by Puccinia triticina. *Mol. Plant Pathol.* **9**, 563–575 (2008).
4) W. Chen, C. Wellings, X. Chen, Z. Kang and T. Liu: Wheat stripe (yellow) rust caused by Puccinia striiformis f. sp. tritici. *Mol. Plant Pathol.* **15**, 433–446 (2014).
5) W. Farha, A. M. Abd El-Aty, M. M. Rahman, J. H. Jeong, H.-C. Shin, J. Wang, S. S. Shin and J.-H. Shim: Analytical approach, dissipation pattern and risk assessment of pesticide residue in green leafy vegetables: A comprehensive review. *Biomed. Chromatogr.* **32**, e4134 (2018).
6) R. M. Caprioli: Imaging Mass Spectrometry: A Perspective. *J. Biomol. Tech.* **30**, 7–11 (2019).
7) A. D. Feenstra, R. L. Hansen and Y. J. Lee: Multi-matrix, dual polarity, tandem mass spectrometry imaging strategy applied to a germinated maize seed: Toward mass spectrometry imaging of an untargeted metabolome. *Analyst (Lond.)* **140**, 7293–7304 (2015).
8) C. Esteve, E. A. Tolner, R. Shyti, A. M. van den Maagdenberg and L. A. McDonnell: Mass spectrometry imaging of amino neurotransmitters: A comparison of derivatization methods and application in mouse brain tissue. *Metabolomics* **12**, 30 (2016).
9) E. Takeo, Y. Sugiura, T. Uemura, K. Nishimoto, M. Yasuda, E. Sugiyama, S. Ohtsuki, T. Higashi, T. Nishikawa, M. Suematsu, E. Fukusaki and S. Shimma: Tandem mass spectrometry imaging reveals distinct accumulation patterns of steroid structural isomers in human adrenal glands. *Anal. Chem.* **91**, 8918–8925 (2019).
10) D. S. Cornett, S. L. Frappier and R. M. Caprioli: MALDI-FTICR imaging mass spectrometry of drugs and metabolites in tissue. *Anal. Chem.* **80**, 5648–5653 (2008).
11) S. Taira, M. Tokai, D. Kaneko, H. Katano and Y. Kawamura-Konishi: Mass spectrometry imaging analysis of location of procymidone in cucumber samples. *J. Agric. Food Chem.* **63**, 6109–6112 (2015).
12) M. Kubicki, M. Lamshöft, A. Lagojda and M. Spiteller: Metabolism and spatial distribution of metalaxyl in tomato plants grown under hydroponic conditions. *Chemosphere* **218**, 36–41 (2019).
13) B. Li, Y. Zhang, J. Ge, K. Liu and P. Li: Sample preparation for mass spectrometry imaging of leaf tissues: A case study on analyte delocalization. *Anal. Bioanal. Chem.* **410**, 7449–7456 (2018).
14) K. Yamamoto, K. Takahashi, L. Caputi, H. Mizuno, C. E. Rodriguez-Lopez, T. Iwasaki, K. Ishizaki, H. Fukaki, M. Ohnishi, M. Yamazaki, T. Masujima, S. E. O'Connor and T. Mimura: The complexity of intercellular localisation of alkaloids revealed by single-cell metabolomics. *New Phytol.* **224**, 848–859 (2019).
15) D. W. Bartlett, J. M. Clough, J. R. Godwin, A. A. Hall, M. Hamer and B. Parr-Dobrzanski: The strobilurin fungicides. *Pest Manag. Sci.* **58**, 649–662 (2002).
16) Y. Feng, Y. Huang, H. Zhan, P. Bhatt and S. Chen: An overview of strobilurin fungicide degradation: Current status and future perspective. *Front. Microbiol.* **11**, 389 (2020).
17) Y. Inoue, T. T. P. Vy, K. Yoshida, H. Asano, C. Mitsuoka, S. Asuke, V. L. Anh, C. J. R. Cumagun, I. Chuma, R. Terauchi, K. Kato, T. Mitchell, B. Valent, M. Farman and Y. Tosa: Evolution of the wheat blast fungus through functional losses in a host specificity determinant. *Science* **357**, 80–83 (2017).
18) Uwe Meier: Growth stages of mono- and dicotyledonous plants: BBCH monograph. *Open Agrar Repositorium, Quedlinburg.*, 2018
19) T. D. Miller: "Growth Stages of Wheat: Identification and Understanding Improve Crop Management," Potash & Phosphate Institute, Norcross, 1992.
20) T. N. Buckley, L. Sack and M. E. Gilbert: The role of bundle sheath extensions and life form in stomatal responses to leaf water status. *Plant Physiol.* **156**, 962–973 (2011).
21) A. Rösch, M. Gottardi, C. Vignet, N. Cedergreen and J. Hollender: Mechanistic understanding of the synergistic potential of azole fungicides in the aquatic invertebrate gammarus pulex. *Environ. Sci. Technol.* **51**, 12784–12795 (2017).
22) I. Kubigsteltig, D. Laudert and E. W. Weiler: Structure and regulation of the Arabidopsis thaliana allene oxide synthase gene. *Planta* **208**, 463–471 (1999).
23) D. A. Bell-Lelong, J. C. Cusumano, K. Meyer and C. Chapple: Cinnamate-4-hydroxylase expression in Arabidopsis. Regulation in response to development and the environment. *Plant Physiol.* **113**, 729–738 (1997).